Realization of Transmission Zeros in Combline Filters Using an Auxiliary Inductively Coupled Ground Plane

Ching-Wen Tang, Yin-Ching Lin, and Chi-Yang Chang, *Member, IEEE*

Abstract—The out-band transmission zeros of the multilayer low-temperature co-fired ceramic bandpass filter are studied in this paper. The design target of this filter, with the passband between 2.3–2.65 GHz (the true application is 2.4–2.483 GHz), is to reject the local oscillator and image signals and, in the mean time, to suppress the harmonic frequency. This filter is a modified three-pole combline filter, which can easily achieve a high rejection rate and low insertion loss. The source–load coupling capacitor incorporation with cross-coupling grounding inductors can generate three transmission zeros. By properly adjusting the inductance values of the inductors between three resonators and ground can easily manipulate the transmission zero at a high-side skirt to suppress the harmonic frequency. The measured results match well with the electromagnetic simulation that evidences the feasibility of the proposed design.

Index Terms—Chip-type component, filter, low-temperature co-fired ceramic (LTCC), multilayer ceramic (MLC).

I. INTRODUCTION

THE high-performance, low-cost, and miniaturized chip-type components using in RF applications are the current trend. The low-temperature co-fired ceramic (LTCC) technology [1]–[6] with the feature of a three-dimensional (3-D) structure can easily integrate these high-frequency circuits into a compact chip-size component.

In the RF front-end, the bandpass filter is one of the most important components. This paper proposes a novel method, which uses inductance coupling among three resonators and can be implemented in the LTCC filter design. Under the consideration of high rejection rate and low insertion loss, the three-pole combline filter [7] with capacitive cross-coupling between input and output ports [8], [9] is chosen. It can generate two transmission zeros at a low-side skirt to reject local and image signals. For the high-side skirt, the inductance values between three resonators and ground can be manipulated to generate an extra transmission zero to suppress the harmonic frequency.

This paper describes an analysis method of out-band transmission zeros of the proposed LTCC bandpass filter. Fig. 1
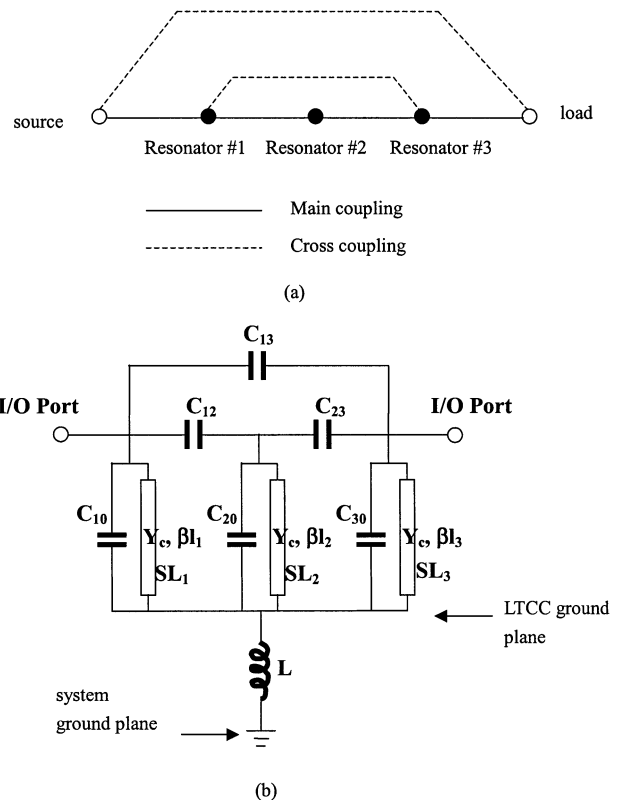
Fig. 1. Coupling schematic and equivalent circuit of the proposed modified combline bandpass filter. (a) Coupling scheme. (b) Equivalent circuit.

shows the coupling scheme and equivalent circuit of the proposed filter. In Fig. 1(a), we use one cross-coupling between resonator #1 and #3 and one source–load cross-coupling to create three finite frequency transmission zeros, two at the lower stopband and one at the upper stopband. Fig. 1(b) shows the equivalent circuit of the proposed filter. In Fig. 1(b), each resonator is formed by a stripline SL_j with a characteristic admittance of Y_c, an electrical length of βl_j, and a grounding capacitor C_{j0}, where subscript j represents the jth resonator. Each resonator is connected to the floating LTCC ground plane that forces the same potential for all resonators at that plane. The LTCC ground plane is then connected to the system ground plane, which is the ground plane of a printed circuit board (PCB) I/O feeding microstrip line. This concept of using series L in the resonator is similar to that of [10]. By tuning the inductance L (between the LTCC ground plane and system ground plane) and cross-coupling capacitor C_{13} properly,

three transmission zeros appeared at proper places. A rigorous synthesis will be difficult on this topology because zeroes are not independent from each other. As was explained in the past literature, adding I/O coupling shifts the transmission zero at infinite frequency downwards, but it does not really add a zero. The measured results of the fabricated multilayer LTCC bandpass filter match well with electromagnetic (EM) simulation.

II. DERIVATION OF THE Y MATRIX

In the analysis of this bandpass filter, the Y-parameter [11] is adopted. According to Fig. 1, the Y matrix of the combline filter can be obtained by following procedures. Firstly, find the Z matrix of the three coupled resonator by cascading the $ABCD$ matrices of three resonators and coupling capacitors. Then series connect it with the grounding inductor L by summing up the Z matrices. After matrix inversion, we have the Y matrix of the combline filter excluding C_{13}. Finally, summing up the Y matrices of cross-coupling capacitor C_{13} and the filter excluding C_{13} gets the result. Here, for simplifying the analysis, let $l_1 = l_3$, $C_{10} = C_{30} = C_1$, $C_{20} = C_2$, $C_{12} = C_{23} = C_3$, and $C_{13} = C_4$ and

$$
\begin{aligned}
Y_{11} = & Y_{22} \\
= & Y_{C4} \\
& + \frac{Y_{C3}^2 + (1 + Y_{C3}Z_L + Y_1 Z_L) \cdot [Y_2 Y_{C3} + Y_1(Y_2 + 2Y_{C3})]}{2Y_{C3} + 4Y_1 Y_{C3} Z_L + Y_2(1 + 2Y_{C3}Z_L + 2Y_1 Z_L)} \\
= & \frac{Y_{N1}}{Y_D}
\end{aligned} \tag{1}
$$

$$
\begin{aligned}
Y_{12} = & Y_{21} \\
= & -Y_{C4} - \frac{Y_{C3}^2 + Z_L(Y_1 + Y_{C3}) \cdot [Y_2 Y_{C3} + Y_1(Y_2 + 2Y_{C3})]}{2Y_{C3} + 4Y_1 Y_{C3} Z_L + Y_2(1 + 2Y_{C3}Z_L + 2Y_1 Z_L)} \\
= & \frac{Y_{N2}}{Y_D}
\end{aligned} \tag{2}
$$

where the admittances of three resonators are $Y_1 = j(\omega C_1 - Y_C \cot(\beta l_1))$, $Y_2 = j(\omega C_2 - Y_C \cot(\beta l_2))$, and $Y_3 = j(\omega C_1 - Y_C \cot(\beta l_1)) = Y_1$. Z_L is the impedance of inductor L, and Y_{C3} and Y_{C4} are the admittances of capacitor C_3 and C_4, respectively. These parameters can be substituted into (1) and (2), and Y_{N1}, Y_{N2}, and Y_D can be obtained as follows:

$$
\begin{aligned}
Y_{N1} = & -\omega^2 \Big\{ C_1 C_2 + 2C_1 C_3 + C_2 C_3 + C_3^2 + C_2 C_4 + 2C_3 C_4 \\
& \quad - \omega^2 L(C_1 + C_3 + 2C_4) \cdot [C_2 C_3 + C_1(C_2 + 2C_3)] \Big\} \\
& + \omega Y_C \cot(\beta l_1) \cdot \Big\{ C_2 [1 - 2\omega^2 L(C_1 + C_3 + C_4)] \\
& \qquad + 2C_3 [1 - \omega^2 L(2C_1 + C_3 + 2C_4)] \\
& \qquad + \omega L(C_2 + 2C_3) Y_C \cot(\beta l_1) \Big\} \\
& - Y_C \cot(\beta l_2) \cdot \Big\{ -\omega(C_1 + C_3 + C_4) + \omega^3 L(C_1 + C_3) \\
& \qquad \cdot (C_1 + C_3 + 2C_4) + Y_C \cot(\beta l_1) \\
& \qquad \cdot [1 - 2\omega^2 L(C_1 + C_3 + C_4) \\
& \qquad + \omega L Y_C \cot(\beta l_1)] \Big\}
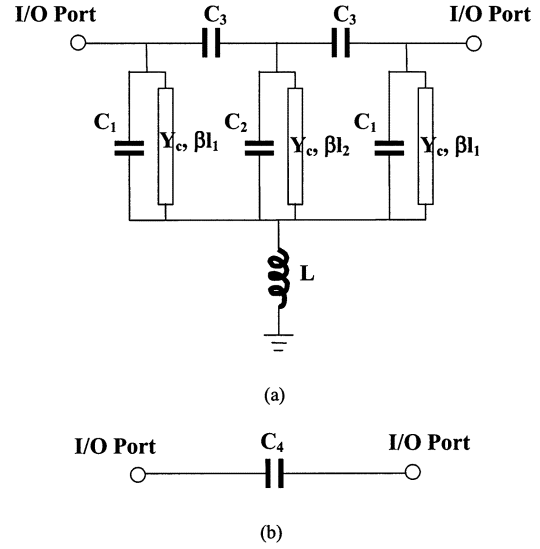\end{aligned} \tag{3}
$$

(a)

(b)

Fig. 2. Separate the cross-coupling capacitor C_4 from the equivalent circuit of Fig. 1 in the analysis of the Y-parameter. (a) Without the cross-coupling capacitor C_4. (b) Cross-coupling capacitor C_4.

$$
\begin{aligned}
Y_{N2} = & \omega^2 \Big\{ C_3^2 + C_2 C_4 + 2C_3 C_4 - \omega^2 L(C_1 + C_3 + 2C_4) \\
& \quad \cdot [C_2 C_3 + C_1(C_2 + 2C_3)] \Big\} + \omega^2 L Y_C \cot(\beta l_1) \\
& \times \Big\{ 2\omega [C_1(C_2 + 2C_3) + C_2(C_3 + C_4) + C_3(C_3 + 2C_4)] \\
& \quad - (C_2 + 2C_3) Y_C \cot(\beta l_1) \Big\} \\
& + \omega Y_C \cot(\beta l_2) \Big\{ -C_4 + \omega^2 L(C_1 + C_3)(C_1 + C_3 + 2C_4) \\
& \qquad + L Y_C \cot(\beta l_1) \\
& \qquad \cdot [-2\omega(C_1 + C_3 + C_4) + Y_C \cot(\beta l_1)] \Big\}
\end{aligned} \tag{4}
$$

$$
\begin{aligned}
Y_D = & +j \Big\{ 2\omega C_3 - 4\omega^2 L C_3 (\omega C_1 - Y_C \cot(\beta l_1)) \\
& \quad + (\omega C_2 - Y_C \cot(\beta l_2)) \cdot [1 + 2\omega L Y_C \cot(\beta l_1) \\
& \qquad - 2\omega^2 L(C_1 + C_3)] \Big\}
\end{aligned} \tag{5}
$$

III. PREDICTION OF THE TRANSMISSION ZEROS BY ADMITTANCE MATRIX

In Section II, the Y-parameter of the proposed bandpass filter has been obtained. Equation (2) can be separated into two parts, as shown in Fig. 2. The first part is the filter without coupling capacitor C_4, as shown in Fig. 2(a). The response of this part shows a transmission zero at the high-side skirt, as shown in Fig. 3. The remainder is the cross-coupling capacitor C_4, as shown in Fig. 2(b). When this capacitor C_4 is connected at the input and output ports of Fig. 2(a), the low-side transmission zeros appear.

Applying the cross-coupling capacitor C_4 to the filter can explain the reason why the proposed multilayer LTCC bandpass filter has three out-band transmission zeros. Fig. 4 explains that the transmission zeros may appear at both sides of passband. The Y-parameter method is extremely fit for analyzing the
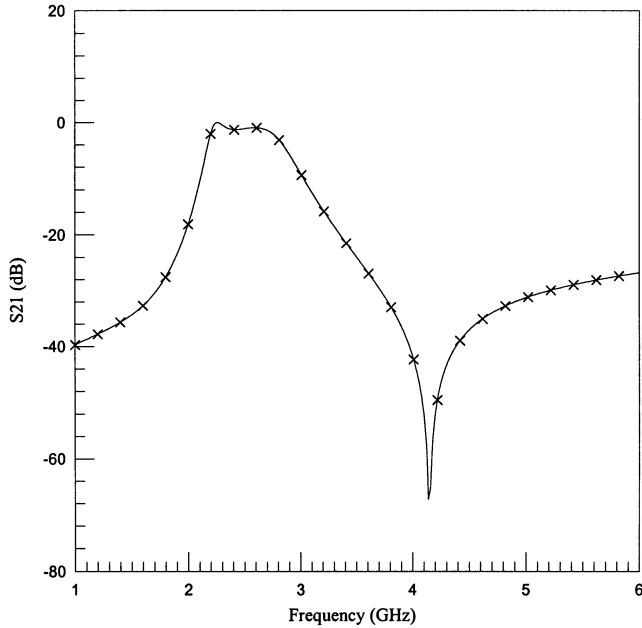
Fig. 3. Response of the filter in Fig. 2(a) with the transmission zero located at the high-side skirt.
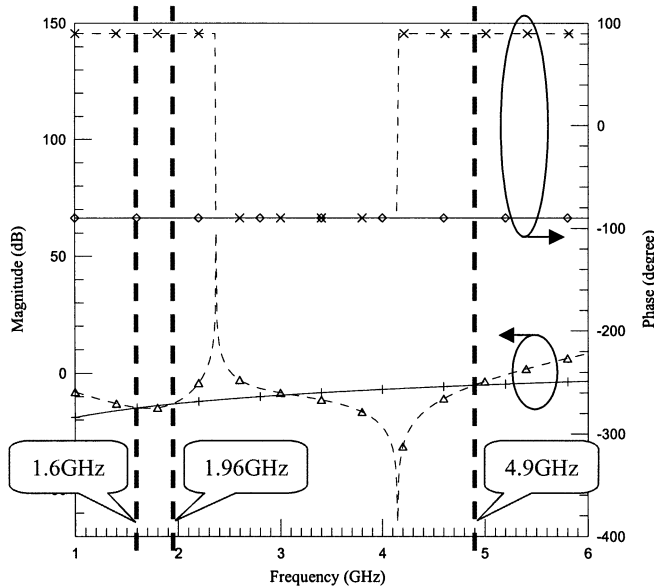

Fig. 4. Applying the Y-parameter to analyze the transmission zeros of the proposed multilayer LTCC bandpass filter (--△-- : the magnitude response of Y_{21} of the filter excluding C_4. --✕-- : the phase response of Y_{21} of the filter excluding C_4. —+— : the magnitude response of Y_{21} of C_4. —◇— : the phase response of Y_{21} of C_4).

out-band transmission zeros. The inductor L (with small inductance value) provides the opposite phase, at the high-side skirt, compared with the circuit without inductor L. The magnitude of Y_{21} of the filter excluding C_4 has two resonant peaks, i.e., the first one at a lower frequency goes upward and the second one at a higher frequency goes downward, as shown in Fig. 4. The transmission zeros occur at the frequencies where Y_{21} of C_4 and Y_{21} of the reminder part of the filter have the same magnitude, but opposite phase. This means that Y_{21} of the whole filter at these points will be zero. The transmission zero points satisfying the above criteria are indicated in Fig. 4.
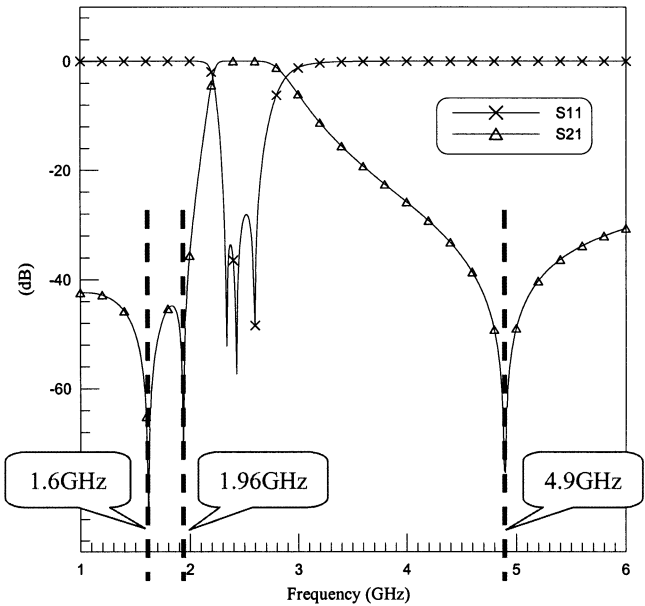

Fig. 5. Simulated result of the multilayer LTCC bandpass filter.

In the 2.4-GHz wireless local area network (LAN) application, the image signal needs to be highly attenuated to maintain the high-quality signal received from the antenna. Moreover, concerning the purity of the transmitted signal, the harmonic frequency also needs to be suppressed. This filter with the characteristics of having two transmission zeros at the low-side skirt can generate a high attenuation rate and suppress all the lower stopband signals. The transmission zero at the high-side skirt can be placed at an exact second harmonic frequency. According to the above-mentioned specification, the modified combline filter has been designed. During the simulation processes, we firstly fine tune each element value in Fig. 1 by the circuit simulator [12]. The corresponding component values in Fig. 1 are $C_{10} = C_{30} = 4.48$ pF, $C_{20} = 2.16$ pF, $C_{12} = C_{23} = 0.77$ pF, and $C_{13} = 0.36$ pF, the length and width are 74 mil × 8 mil for SL_1 and SL_3 and 115 mil × 8 mil for SL_2, respectively, and $L = 0.04$ nH. The ceramic substrate of the LTCC has the dielectric constant of 7.8 and stripline ground plane spacing of 21.6 mil. After circuit simulation, convert these values into the LTCC structure and simulate via an EM simulator. The circuit simulator's simulated response of the bandpass filter is shown in Fig. 5.

IV. ANALYSIS BY EM SIMULATION

Considering the practical environment, the LTCC bandpass filter is mounted on the pad of a PCB. The overall performance should include the parasitic of the PCB, as shown in Fig. 6(a). Owing to the small value of L, as obtained in Section III, the L can be easily accomplished by adjusting the size and number of plated through-holes on the PCB. Practical realization of the multilayer bandpass filter can be simplified into three parts, i.e., the inductor's part, the stripline's part, and the capacitor's part, as shown in Fig. 6(a).
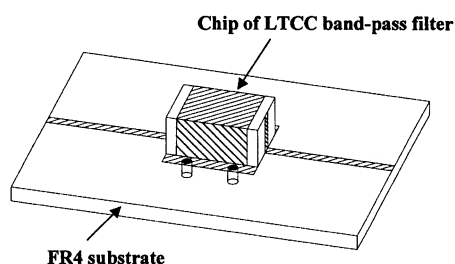
Part I, i.e., the inductor's part, can be realized by four plated through-holes on the PCB and LTCC buffer layer, which is lo-
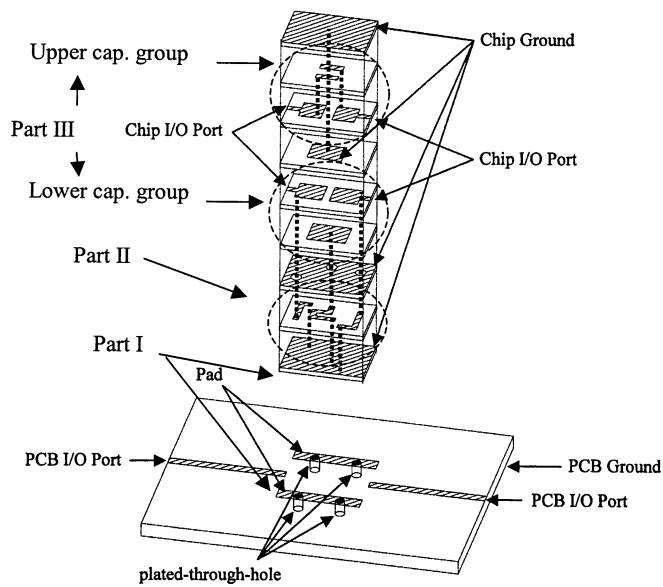
(a)
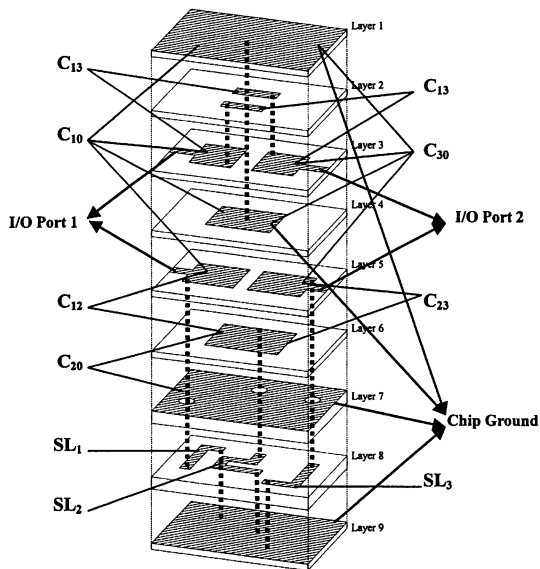
(b)

(c)

Fig. 6. 3-D structure of proposed modified combline filter. (a) 3-D view of multilayer LTCC filter and PCB environment. (b) Detailed locations of each component in the ceramic part. (c) The LTCC bandpass filter has been soldered on the PCB.

cated at the bottom of the chip, to accomplish the proper L value. Part II, i.e., the stripline's part, are located in the middle of the
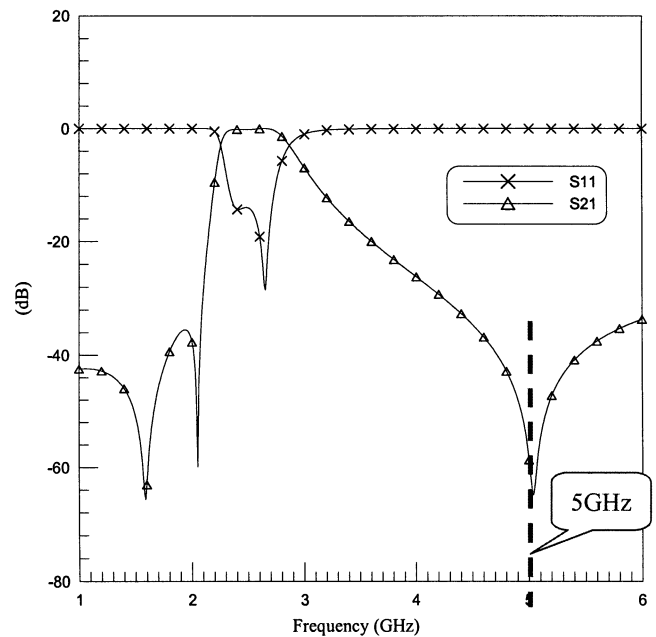

Fig. 7. Simulated response of an LTCC filter mounted on a PCB, as shown in Fig. 6(c).

chip and should be meandered to fit the chip size. Part III, i.e., the capacitor's part, are located on the top of the chip. This arrangement is a modularized method and can simplify the design of the 3-D structure.

Fig. 6(b) is the architecture of ceramic part, which does not include the PCB inductor. During the processes of practical design, the whole structure involves the PCB part, can exhaust much more computing time during the fully 3-D EM simulation [13], and is difficult to fine tune. The chip part, as shown in Fig. 6(b), can be developed independently using a two-and-one-half-dimensional (2.5-D) EM simulator [14]. It is helpful to design the capacitor's and stripline's parts separately before connecting them.

As shown in Fig. 6(a), from top to bottom, the capacitor's part is located from layer 1 to 7. It can be further separated into two groups, layer 1 to 4, and layer 4 to 7. Layer 4 is one of the ground plane in the chip because it is connected to the top ground plane, which is layer 1. The upper group, from layer 1 to 4, can generate C_{13} and a portion of C_{10} and C_{30}. The lower group, from layer 4 to 7, can implement C_{12}, C_{23}, and C_{20} and the remainder portion of C_{10} and C_{30}. The detail capacitor locations are depicted in Fig. 6(b).

In Part II, i.e., the stripline's part, the short-circuit transmission lines of the combline resonators are connected to the bottom chip ground, which is layer 9. This LTCC filter will be mounted on the PCB by connecting the chip ground, layer 1 and 9, to the pads on the PCB. The PCB pads connect the PCB ground plane through plated through-holes. The parasitic through-hole inductance can be adopted in our filter design and simplify the multilayer structure. Fig. 6(a) and (b) shows the filter with the dimensions not to the scale. Fig. 6(c) shows the LTCC bandpass filter soldered on the PCB.

The PCB mounting environment, as shown in Fig. 6(c), can be simulated by the fully 3-D EM simulator *HFSS* [13]. The simulated results are shown in Fig. 7. Simulation in Fig. 7 is based
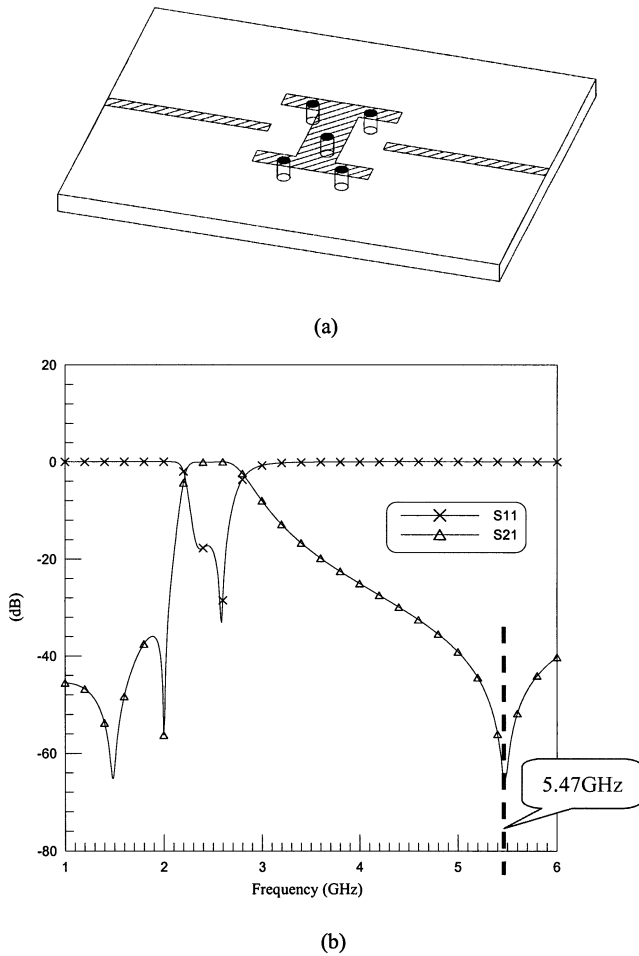
(a)

(b)

Fig. 8.   LTCC bandpass filter mounted on a PCB, which has an extra plated through-hole at the center of the grounding pad. (a) 3-D view of the PCB grounding pad. (b) Simulated filter response.

on a popular FR4 PCB substrate with a thickness of 0.4 mm and a dielectric constant of 4.47. The parasitic PCB through-hole inductance generates a higher stopband transmission zero at 5 GHz.

Here, we have analyzed three parasitic effects, namely, the: 1) through-hole inductance; 2) microstrip gap; and 3) buffer layer thickness, which can influence the location of three transmission zeros of the LTCC filter mounted on a PCB. The discussions are as follows.

A. Effect of Parasitic Through-Hole Inductance

The parasitic through-hole inductance L, as shown in Fig. 1, can be controlled by a number of plated through-holes. If the number of plated through-holes increases, the parasitic through-hole inductance L decreases and the second resonance frequency of Y_{21} excluding C_4 in Fig. 4 also increases, which causes the transmission zero shift to a higher frequency. Fig. 8(a) shows an additional plated through-hole that appeared in the middle of the PCB grounding pad. This extra plated through-hole causes the original transmission zero to shift from 5 to 5.47 GHz, as shown in Fig. 8(b).
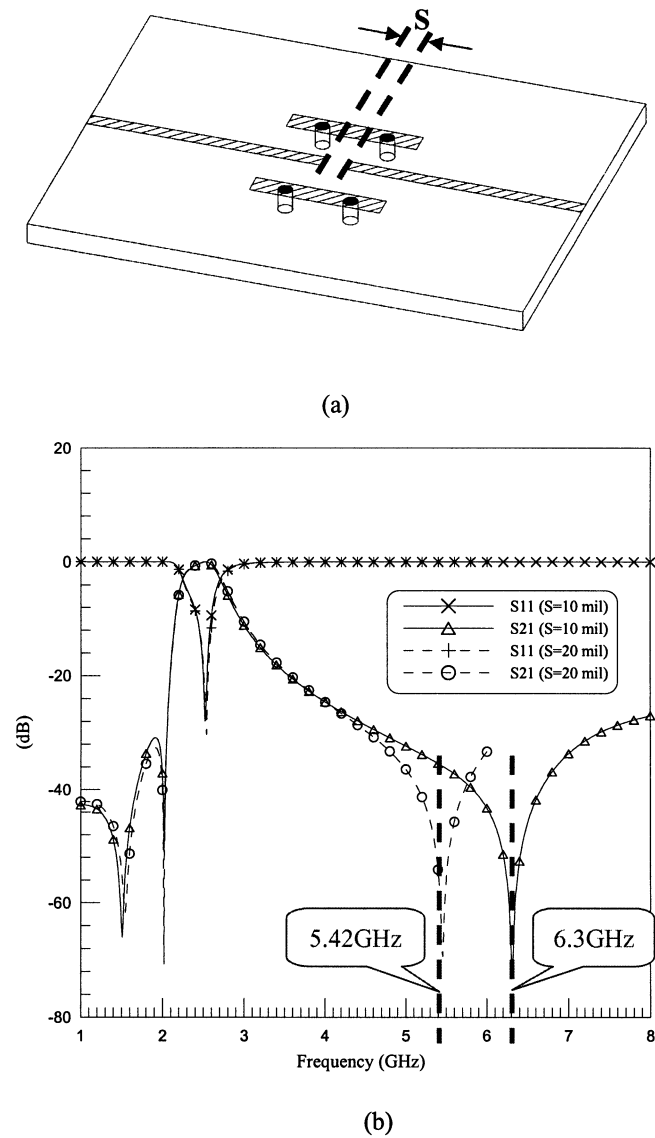

(a)

(b)

Fig. 9.   Multilayer LTCC bandpass filter mounted on a PCB with microstrip gap S. (a) 3-D view of the PCB layout. (b) Simulated responses corresponding to microstrip gap S of 10 and 20 mil.

B. Effect of Microstrip Gap

This location of the transmission zero at a high-side skirt is also controllable by adjusting the cross-coupling capacitor C_4 in Fig. 1. According to Fig. 4, the larger the cross-coupling capacitance C_4, the curve of $Y_{21\_}C_4$ (dB) (—+—) moves to a higher level so that the transmission zero (the intersection point) at the high-side skirt moves to a higher frequency. Fig. 9(a) shows the 3-D view of the PCB layout. The microstrip gap S in Fig. 9(a) enhances the cross-coupling capacitance. The simulated responses of the LTCC filter with coupling gaps S equals 10 and 20 mil, and are shown in Fig. 9(b). The extra gap capacitance moves the original transmission zero from 5 GHz to 6.3 and 5.42 GHz, respectively.

C. Effect of Buffer Layer Thickness

Another parameter, the buffer layer thickness H of the LTCC bandpass filter, as shown in Fig. 10(a) (i.e., the dummy layer between the chip's ground plane and the surface of the PCB), also
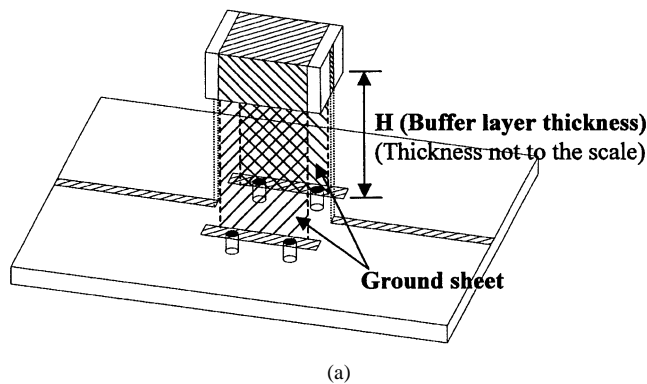
(a)
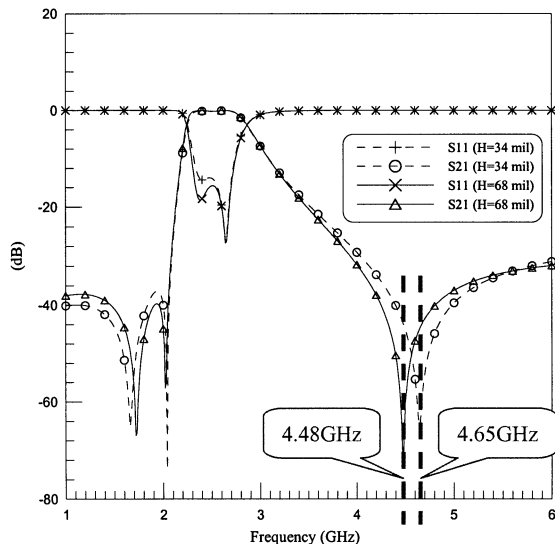
(b)

Fig. 10. Effect of buffer layer thickness H of the multilayer LTCC bandpass filter. (a) 3-D view of the LTCC filter mounted on a PCB. (b) Simulated response corresponding to H equals 34 and 68 mil.

influences the position of the transmission zero at the high-side skirt. Higher buffer layer thickness H causes a larger inductance L value in Fig. 1. The increased value of L moves Y_{21}'s second resonant frequency in Fig. 4 to a lower frequency and, as a result, the transmission zero at the high-side skirt shifts downward. Fig. 10(b) shows the simulated result of the LTCC filter with the buffer layer thickness H corresponding to 34 and 68 mil, respectively. This extra inductance moves the original transmission zero at 5 GHz to 4.65 and 4.48 GHz, respectively.

V. MEASURED RESULTS

According to the analysis in the above section, the chip-type LTCC bandpass filter has been fabricated using Dupont 951 (with the dielectric constant 7.8 and loss tangent = 0.0045), as shown in Fig. 11(a). The LTCC filter is designed based on the buffer layer thickness of 3.6 mil and the PCB mounting environment similar to Fig. 6(c). The chip size is 3.2 mm × 2.5 mm × 1.2 mm. Fig. 11(b) shows the measured results of the fabricated LTCC bandpass filter. The passband insertion loss (between 2.4 and 2.5 GHz) is less than 1.67 dB. The designed out-band transmission zeros are at 1.62, 1.97, and 4.92 GHz, respectively. The measured metal's thickness of the fabricated LTCC filter is merely 5 μm, which will cause the passband's
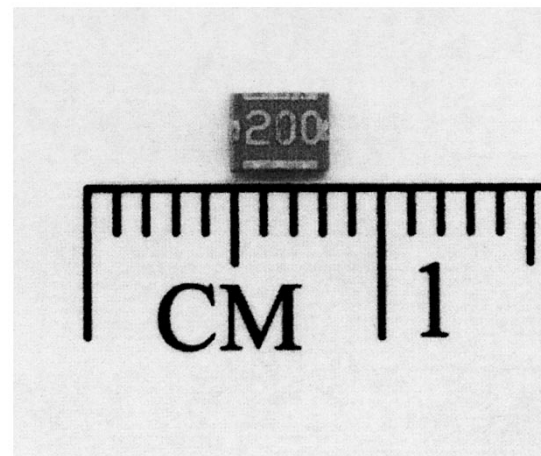
(a)
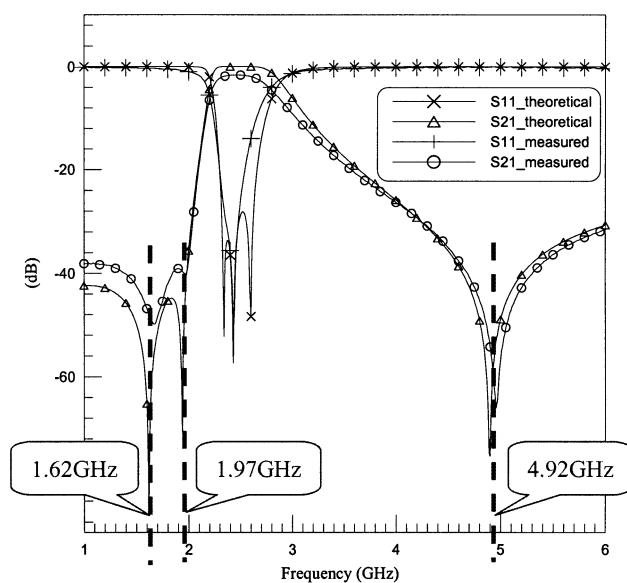
(b)

Fig. 11. Fabricated multilayer LTCC bandpass filter. (a) Photograph and (b) measured performance where the mounting environment is similar to Fig. 6.

insertion loss to be a little higher. As shown in Fig. 11(b), the measured results match well with the theoretical one, except for the insertion loss. The measured insertion loss is higher than the theoretical result because the substrate and metal losses are not included in the simulation for simulation speed consideration.

VI. CONCLUSION

A novel LTCC-multilayer ceramic (MLC) bandpass filter has been developed. The proposed cross-coupling scheme has successfully generated three desired finite frequency transmission zeros. The Y-parameter analysis has precisely predicted the locations of them. The equivalent circuit and detail structured of this bandpass filter have been given. The designed chip-type bandpass filter has been fabricated with a multilayer configuration. The measured performance agrees well with the simulation. The passband's insertion loss was better than −1.67 dB, and the out-band transmission zeros match well with simula-

tion. The results show the validity of the proposed structure and design method.

ACKNOWLEDGMENT

REFERENCES

[1] J. Muller and H. Thust, "3D-intergration of passive RF-components in LTCC," in *Pan Pacific Microelectronic Symp. Dig.*, 1997, pp. 211–216.

[2] C. Q. Scrantom and J. C. Lawson, "LTCC technology: Where we are and where we're going—II," in *IEEE MTT-S Int. Microwave Symp. Dig.*, 1999, pp. 193–200.

[3] Y. Rong, K. A. Zaki, M. Hageman, D. Stevens, and J. Gipprich, "Low temperature cofired ceramic (LTCC) ridge waveguide bandpass filters," in *IEEE MTT-S Int. Microwave Symp. Dig.*, June 1999, pp. 1147–1150.

[4] J. W. Sheen, "LTCC–MLC duplexer for DCS-1800," *IEEE Trans. Microwave Theory Tech.*, vol. 47, pp. 1883–1890, Sept. 1999.

[5] D. Heo, A. Sutono, E. Chen, Y. Suh, and J. Laskar, "A 1.9 GHz DECT CMOS power amplifier with fully integrated multilayer LTCC passives," *IEEE Microwave Wireless Comp. Lett.*, vol. 11, pp. 249–251, June 2001.

[6] W. Y. Leung, K. K. M. Cheng, and K. L. Wu, "Design and implementation of LTCC filters with enhanced stop-band characteristics for Bluetooth applications," in *Proc. Asia–Pacific Microwave Conf.*, Dec. 2001, pp. 1008–1011.

[7] G. L. Matthaei, L. Young, and E. M. T. Jones, *Microwave Filters, Impedance Matching Networks, and Coupling Structures*. Norwood, MA: Artech House, 1980.

[8] S. Amari, "Direct synthesis of folded symmetric resonator filters with source–load coupling," *IEEE Microwave Wireless Comp. Lett.*, vol. 11, pp. 264–266, June 2001.

[9] K. A. Zaki, C. Chen, and A. E. Atia, "A circuit model of probes in dual-mode cavities," *IEEE Trans. Microwave Theory and Tech.*, vol. 36, pp. 1740–1746, Dec. 1988.

[10] J. S. Lim and D. C. Park, "A modified Chebyshev bandpass filter with attenuation poles in the stopband," *IEEE Trans. Microwave Theory Tech.*, vol. 45, pp. 898–904, June 1997.

[11] D. M.David M. Pozar, *Microwave Engineering*, 2nd ed. New York: Wiley, 1998.

[12] *Advanced Design System User Manual*, Agilent Technol., Palo Alto, CA, 2002.

[13] *HFSS User Manual*, Ansoft, Pittsburgh, PA, 2002.

[14] *Em User's Manual*, Sonnet Software Inc., Liverpool, NY, 2002.
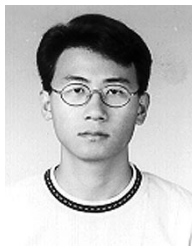
Ching-Wen Tang received the B.S. degree in electronic engineering from Chung Yuan Christian University, Chungli, Taiwan, R.O.C., in 1991, and the M.S. and Ph.D. degrees in communication engineering from the National Chiao Tung University, Hsinchu, Taiwan, R.O.C., in 1996 and 2002, respectively.

In 1997, he joined the RF Communication Systems Technology Department, Computer and Communication Laboratories, Industrial Technology Research Institute (ITRI), Hsinchu, Taiwan, R.O.C., as a RF Engineer, where he developed LTCC–MLC RF components. In 2001, he joined Phycomp Taiwan Ltd., Kaohsiung, Taiwan, R.O.C., as a Project Manager, where he continues to develop LTCC components and modules. Since February 2003, he has been with the Department of Communication Engineering, National Chung Cheng University, Chiayi, Taiwan, R.O.C., where he is currently an Assistant Professor. His research interests include microwave and millimeter-wave planar-type and multilayer circuit design, and the analysis and design of thin-film components.
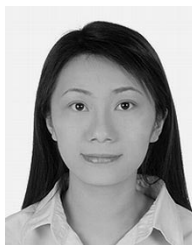
Yin-Ching Lin was born on August 27, 1978, in Taiwan, R.O.C. She received the B.S. and M.S. degrees in communication engineering from the National Chiao Tung University, Taiwan, R.O.C., in 2000 and 2002, respectively, and is currently working toward the Ph.D. degree in communication engineering at the National Chiao Tung University.

She is currently an RF Engineer with the Gincom Technology Corporation, Taiwan, R.O.C., where she designs LTCC RF passive components and LTCC modules for wireless local area network (LAN) applications. Her postgraduate research is concentrated on microwave circuits and LTCC RF circuit design.

Chi-Yang Chang (S'88–M'95) received the B.S. degree in physics and M.S. degree in electrical engineering from the National Taiwan University, Taiwan, R.O.C., in 1977 and 1982, respectively, and the Ph.D. degree in electrical engineering from The University of Texas at Austin, in 1990.

From 1979 to 1980, he was a Teaching Assistant with the Department of Physics, National Taiwan University. From 1982 to 1988, he was an Assistant Researcher with the Chung-Shan Institute of Science and Technology (CSIST), where he was in charge of development of microwave integrated circuits (MICs), microwave subsystems, and millimeter-wave waveguide E-plane circuits. From 1990 to 1995, he had rejoined CSIST as an Associate Researcher, where he was in charge of development of uniplanar circuits, ultra-broad-band circuits, and millimeter-wave planar circuits. In 1995, he joined the faculty of the Department of Communication, National Chiao Tung University, Hsinchu, Taiwan, R.O.C., as a Professor. His research interests include microwave and millimeter-wave passive and active circuit design, planar miniaturized filter design, and monolithic-microwave integrated-circuit (MMIC) design.